Title: The multi-Siglec inhibitor AL009 reprograms suppressive macrophages and activates innate and adaptive tumor immunity[1]

Authors: Sam C. Nalle,[2] Helen Lam, Ling Leung, Spencer Liang, Daniel Maslyar, Arnon Rosenthal

Affiliation:

Alector, Inc., South San Francisco, CA, USA.

Running title: AL009 reprograms macrophages to drive anti-tumor immunity

Abstract:

Sialic acid–binding immunoglobulin-type lectins (Siglecs) are cell surface receptors that regulate innate and adaptive immunity, with inhibitory Siglecs promoting immune tolerance. In the tumor microenvironment, overexpression of sialic acid glycans exploits inhibitory Siglec signaling, leading to a cancer-permissive phenotype. AL009 is an engineered Siglec-9-Fc fusion molecule that functions as a sialic acid trap and reprograms suppressive macrophages to activate an anti-tumor immune response. AL009 treatment of human myeloid-derived suppressor cells, an in vitro model of tumor-associated macrophages, resulted in an increase in proinflammatory cytokines and chemokines, changes in cell surface markers, and potent relief of T cell inhibition in a co-culture assay. In syngeneic mouse (*Mus musculus*) tumor models, AL009 engineered with a mouse Fc (AL009m) reduced tumor growth as a monotherapy and in combination with the checkpoint inhibitor anti-PD-L1. In addition, AL009m synergized with the tumor-targeting therapy anti-TRP1 to reduce lung nodules in the B16-F10 intravenous model. Pharmacodynamic marker analysis in syngeneic and humanized mouse tumor models supported an AL009 mechanism of action based on reprogramming tumor-associated macrophages and enhanced T cell activation. Future clinical studies are warranted to further elucidate the safety and efficacy of AL009.

INTRODUCTION

Sialic acid–binding immunoglobulin-like lectins (Siglecs) are immune regulatory molecules that interact with sialic acid residues in the glycocalyx to modulate innate and adaptive immune response (1-3). Inhibitory Siglecs, such as Siglec-3, -5, -7, -9, and -10, contain an immunoreceptor tyrosine-based inhibition motif that recruits tyrosine phosphatases (such as SHP1 and SHP2) involved in dampening the immune response to maintain homeostasis (1, 2, 4, 5). This is particularly important for recognition of self and resolution of inflammation (6). However, some tumors have exploited this process by overexpressing sialic acid ligands on the tumor cell surface to engage inhibitory Siglecs and evade immune detection, thus promoting an immunosuppressive, cancer-permissive phenotype (1, 5, 7, 8). Disrupting the signaling between immune-inhibitory Siglecs and their sialic acid ligands on hypersialylated cancer cells could confer a therapeutic benefit, making both Siglecs and their sialic acid ligands attractive targets for cancer immunotherapies (2, 8, 9).

Siglecs are expressed on various immune cells but predominantly on myeloid cells, including macrophages and myeloid-derived suppressor cells (MDSCs) (2, 5). The immunoregulatory activity of macrophages, whether proinflammatory or immunosuppressive, can change depending on the chemokines, cytokines, and enzymes in the surrounding environment, with tumor-associated macrophages (TAMs) being primarily immunosuppressive due to the nature of the tumor microenvironment (TME) (5, 10-13). TAMs are not only influenced by the TME but also contribute to the immunosuppressive signaling therein by releasing anti-inflammatory chemokines and cytokines, such as IL-10 and TGF-β, which ultimately lead to T cell inactivation (10, 13). Cell surface markers can be used to monitor the current immunomodulatory status of macrophages; MHC-II, CD80, and CD86 are increased on proinflammatory macrophages, while

48 suppressive macrophages display elevated CD163 and CD206 (5, 13-15). TAM infiltration into
49 tumors has been associated with worse prognosis, particularly when high levels of Siglecs are
50 displayed (16, 17).

51 Targeted therapeutics designed to reprogram TAMs from an immunosuppressive to a
52 proinflammatory phenotype are currently being investigated (11). Thus far, antibodies against
53 macrophage receptor with collagenous structure (MARCO), the leukocyte immunoglobulin-like
54 receptor B (LILRB) family, Clever-1, and P-selectin glycoprotein ligand-1 (PSGL-1), as well as
55 CD40 agonists, have all shown potential in converting TAMs into proinflammatory effectors
56 (18-22). Interferon gamma (IFNɣ) has also shown potential to skew macrophages towards a
57 proinflammatory phenotype (15, 18, 23). The immunosuppressive characteristic of inhibitory
58 Siglecs along with their expression on TAMs make them ideal targets to modulate macrophage
59 function. However, since multiple inhibitory Siglecs are expressed on TAMs, broad targeting is
60 required to effectively interrupt immunosuppressive Siglec signaling (4, 5).

61 Here, we present data on AL009, an engineered multi-Siglec inhibitor that functions as a sialic
62 acid trap and reprograms suppressive macrophages to activate an anti-tumor immune response.
63 In vitro, AL009 effectively reprograms suppressive macrophages, as demonstrated by changes in
64 cell surface markers as well as increased secretion of proinflammatory cytokines. In animal
65 tumor models, monotherapy with AL009 or combination therapy with AL009 and anti-PD-L1 or
66 anti-TRP1 reduced tumor burden. Taken together, these data support further investigation of
67 AL009 as a targeted immunotherapy across a broad range of tumors high in Siglec-expressing
68 TAMs.
69

70 **MATERIALS AND METHODS**

71 **Study design**

72 The objective of this study was to evaluate the activity of AL009 in vitro and in mouse tumor
73 models. Experiments were designed to elucidate the role of AL009's Siglec-9 extracellular
74 domain (ECD) and its engineered fragment crystallizable (Fc) region, as well as its interactions
75 with and impact on human myeloid cells. Additionally, AL009 pharmacodynamics and efficacy
76 were tested in mouse models.

77 **Animals and reagents**

78 C57BL/6 mice harboring a BAC-expressing human Siglec-3, -7, and -9 were generated and
79 maintained by Alector. Expression of human Siglecs was confirmed by flow cytometry. Mice
80 were maintained by crossing Tg^{het} mice with wildtype C57BL/6 mice, and all mice used in
81 studies were Tg^{het} mice. Anti-PD-L1 was produced at Alector based on a reported sequence.
82 Siglec Fcs and isotype control antibodies were produced at Alector unless otherwise stated. In
83 mouse syngeneic tumor studies, a chimeric form of AL009 was produced with a mouse IgG2a Fc
84 (AL009m). huNOG-EXL humanized mice were purchased from Taconic Biosciences
85 (Germantown, NY) and housed at Alector.

86 **Cell binding competition assay with AL009**

87 MDSCs were generated from healthy human donors by differentiation of $CD14^+$ monocytes
88 isolated using a RosetteSep human monocyte enrichment kit (STEMCELL Technologies). In
89 order to generate MDSCs, $CD14^+$ monocytes were cultured for 7 days in Roswell Park Memorial
90 Institute media containing 10-ng/mL human granulocyte-macrophage colony-stimulating factor
91 and 10-ng/mL human IL-6 (PeproTech). For cell binding competition with AL009, MDSCs were

92 incubated with titrating amounts of AL009, followed by incubation with Siglec-3, -5, -7, -9, or -
93 10 mouse IgG1 Fc fusion molecules. Bound Siglec-3, -5, -7, -9, and -10 Fcs were assessed by
94 detecting with an anti-mouse IgG-specific secondary (Thermo Fisher) and analyzed via flow
95 cytometry (BD Biosciences).

96 **Glycan array**

97 We assessed binding to a library of 300 glycan structures for Fc fusion proteins sourced from a
98 commercial vendor (R&D Systems) composed of a fusion of Siglec-3, -5, -7, -9, -10, or -15
99 ECDs with a human IgG1 Fc. Siglec fusion proteins and control human IgG1 were assessed for
100 glycan binding on the Glycan-300 (RayBiotech). The staining and analysis were performed as a
101 service by RayBiotech using the manufacturer's protocol. Briefly, the recombinant proteins were
102 incubated with the glycan array for 2 to 3 hours, followed by detection with anti-hIgG biotin and
103 streptavidin-Cy3. Samples were read and fluorescence was normalized across samples. For
104 blocking experiments, AL009 and mIgG1 or mIgG1 alone were applied first before incubation
105 with Siglec Fcs and human IgG.

106 **MDSC stimulation and RNAseq analysis of MDSCs treated with AL009**

107 MDSCs were treated with AL009 for 48 hours at 37° C and cell surface markers and cytokine
108 production were analyzed via flow cytometry and LEGENDplex (Biolegend), respectively. For
109 RNAseq analysis, MDSCs were treated with 10 µg/mL of AL009 for 24 hours. Cells were
110 harvested and pelleted, followed by resuspension in RLT buffer (Qiagen). RNA was extracted
111 with the RNeasy Plus Microkit (Qiagen). Illumina compatible libraries were created using
112 Lexogen QuantSeq 3' mRNA-Seq Library Prep Kit FWD and sequenced on a Nextseq P2.

113 **MDSC–T cell co-culture**

114 The activity of AL009 was evaluated alongside several different functional Siglec antibodies in a
115 MDSC–T cell co-culture assay. MDSCs were harvested and co-cultured with autologous $CD8^+$ T
116 cells in the presence of Dynabeads Human T-activator CD3/CD28 (Thermo) and either a Siglec-
117 Fc fusion or antibodies. Proliferation via carboxyfluorescein succinimidyl ester (Thermo Fisher)
118 dilution and cytokine production via LEGENDplex were assessed after 3 to 5 days.

119 **MDSC stimulation with plate-bound IgG and anti-TREM1/anti-TREM2**

120 MDSCs were stimulated with plate-bound human IgG1 with or without 10-µg/mL Siglec-9 ECD
121 co-incubation for 48 hours followed by analysis of TNF production (Meso Scale Discovery).
122 Separately, MDSCs were stimulated with anti–triggering receptor expressed on myeloid cells 1
123 (TREM1) or anti–triggering receptor expressed on myeloid cells 2 (TREM2) agonistic antibodies
124 with or without Siglec-9 ECD for 48 hours followed by analysis of TNF production.

125 **Fcγ receptor blockade**

126 MDSCs were incubated with the 10-µg/mL FcγRIIa (clone IV.3)- or FcγRIIb (clone 2B6)-
127 blocking antibodies alone or in combination for 30 minutes on ice, followed by treatment with
128 3.3-µg/mL AL009 for 24 hours at 37° C and analysis of cell surface markers by flow cytometry.

129 **Specific binding of AL009**

130 For peripheral immune cell binding specificity, healthy human blood was incubated with AF647-
131 labeled AL009 using SiteClick reagents (Thermo Fisher) followed by analysis via flow
132 cytometry. For myeloid binding, healthy human monocytes from peripheral blood, M0
133 macrophages differentiated from human monocytes with 50-ng/mL human M-CSF, M1
134 macrophages differentiated from human monocytes with 50-ng/mL M-CSF, 100-ng/mL

135 lipopolysaccharide (InvivoGen), and 50-ng/mL IFNγ (PeproTech), or MDSCs, were incubated
136 with AF647-labeled AL009 followed by analysis via flow cytometry.

137 **Biodistribution of AL009**

138 Female C57BL/6 mice bearing established subcutaneous MC38.NCI.TD1 murine colon
139 carcinoma were injected intravenously with 10-mg/kg AF647-labeled AL009m. Ex vivo
140 fluorescence imaging using the IVIS Spectrum imaging system was performed on liver, spleen,
141 heart, and lungs collected from each mouse at 1, 6, 24, 48, and 96 hours post injection. Three
142 animals were imaged per time point.

143 **Effect of AL009 in mouse models**

144 The MC38 and B16-F10 cell lines were purchased from American Type Culture Collection. The
145 E0771 cell line was purchased from MI Bioresearch. Female S3/7/9 Tg mice that were 7 to 12
146 weeks old were implanted with MC38 or E0771 cells subcutaneously in the flank region at a
147 density of 1.0×10^5 or 4.0×10^5 cells per mouse, depending on the model. When tumors reached
148 an average volume of ~100 mm^3, mice were randomized into treatment groups and dosing was
149 initiated. Mice received intraperitoneal injections of 10- to 20-mg/kg AL009m or isotype control
150 with or without 3-mg/kg anti-PD-L1 twice per week for 3 weeks. Tumors were measured twice
151 per week with calipers. For the B16-F10 intravenous model, 1.5×10^5 B16-F10 cells were
152 administered via intravenous injection. Mice were treated with 27-µg/mouse anti-TRP1
153 (BioXCell) on day 1 in addition to 10-mg/kg AL009m or isotype control on days 1, 4, 7, 10, and
154 13. A satellite group of animals was dosed only with control antibodies, and several mice in this
155 group were euthanized every 2 days starting on day 9 to assess lung nodules. When the satellite
156 group reached 50 to 100 lung nodules, the remaining experimental groups were euthanized for
157 analysis. Statistical testing was performed by 2-way Student's t-test.

158 **Pharmacodynamic biomarkers**

159 Siglec-3/7/9 BAC Tg mice were implanted with E0771 tumors and randomized for treatment as
160 described above. The mice received intraperitoneal 20-mg/kg AL009m or isotype control on
161 days 0, 4, and 7, and were sacrificed on day 8. Splenic and tumor tissues were mechanically
162 dissociated and passed through a 70-μm filter to obtain single-cell suspensions. Peripheral blood
163 was treated with ammonium-chloride-potassium lysis buffer to lyse red blood cells and washed
164 with phosphate-buffered saline. Cell surface markers on immune cell subsets were analyzed by
165 flow cytometry. In order to identify immune cell subsets, CD3+ T cells were plotted on the y-
166 axis and CD11b+ myeloid cells were plotted on the x-axis, with further subgating occurring from
167 there.

168 For pharmacodynamic analysis of humanized mice, 14- to 16-week-old female huNOG-EXL
169 mice were implanted with A375 melanoma cells subcutaneously in the flank region at a density
170 of with 3.0×10^6 cells per mouse. When tumors reached an average volume of 200 to 400 mm^3,
171 mice received intraperitoneal injections of 10-mg/kg AL009 or isotype control on days 0 and 3
172 and were sacrificed 24 hours later. Cell surface markers on immune cells subsets were analyzed
173 by flow cytometry.

174 **Statistical analyses**

175 Statistical analysis was performed using GraphPad Prism v9. Data are displayed as mean ± SEM.
176 A 2-tailed t-test was used for comparisons between 2 groups. A 1-way ANOVA followed by the
177 Holm-Sidak method of multiple comparisons was used for comparisons of more than 2 groups.
178 A p value of < 0.05 was considered significant.

179 **Study approval**

180 All in-house animal studies were reviewed by, approved by, and performed in compliance with
181 Alector's Institutional Animal Care and Use Committee protocols. Outsourced studies were
182 conducted in accordance with the applicable Covance or Charles River Laboratories standard
183 operating procedures, which approved these studies.

184 **RESULTS**

185 **AL009 displays specific blocking between inhibitory Siglecs and their ligands**

186 AL009 is composed of a Siglec-9 ECD and an engineered Fc to localize the therapeutic to
187 immune cells and promote cooperative binding of the ECD. Given the redundancy of inhibitory
188 Siglecs, an effective therapeutic would require broad blocking between multiple inhibitory
189 Siglecs and their respective ligands. To assess the degree to which AL009 could disrupt Siglec-
190 ligand binding on MDSCs, the binding between Siglec-3, -5, -7, -9, and -10 Fc fusion proteins
191 and human MDSCs was quantified in the presence of increasing concentrations of AL009. With
192 all the Siglec Fcs tested, an AL009 dose-dependent decrease in binding was observed,
193 demonstrating a broadly effective blockade of ligand recognition on cells (Fig. 1A). In order to
194 assess specific ligand blockade, a biochemical blocking assay using AL009 was established with
195 a glycan array containing over 100 sialic acids. Using this assay format, AL009 blocked binding
196 of known sialic acids recognized by inhibitory Siglecs -3, -5, and -7 (Fig. 1B-D). As the binding
197 portion of AL009 is composed of a Siglec-9 ECD, Siglec-9 binding relative to other inhibitory
198 Siglecs was evaluated side by side using a glycan array. Siglec-9 displayed an extensive sialic
199 acid binding profile compared to other inhibitory Siglecs (Fig. S1), helping to explain the ability
200 of AL009 to block ligands recognized by multiple Siglecs on MDSCs. Overall, these results
201 demonstrate that AL009 possesses the ability to block specific ligand binding of at least 5
202 inhibitory Siglecs present on myeloid cells.

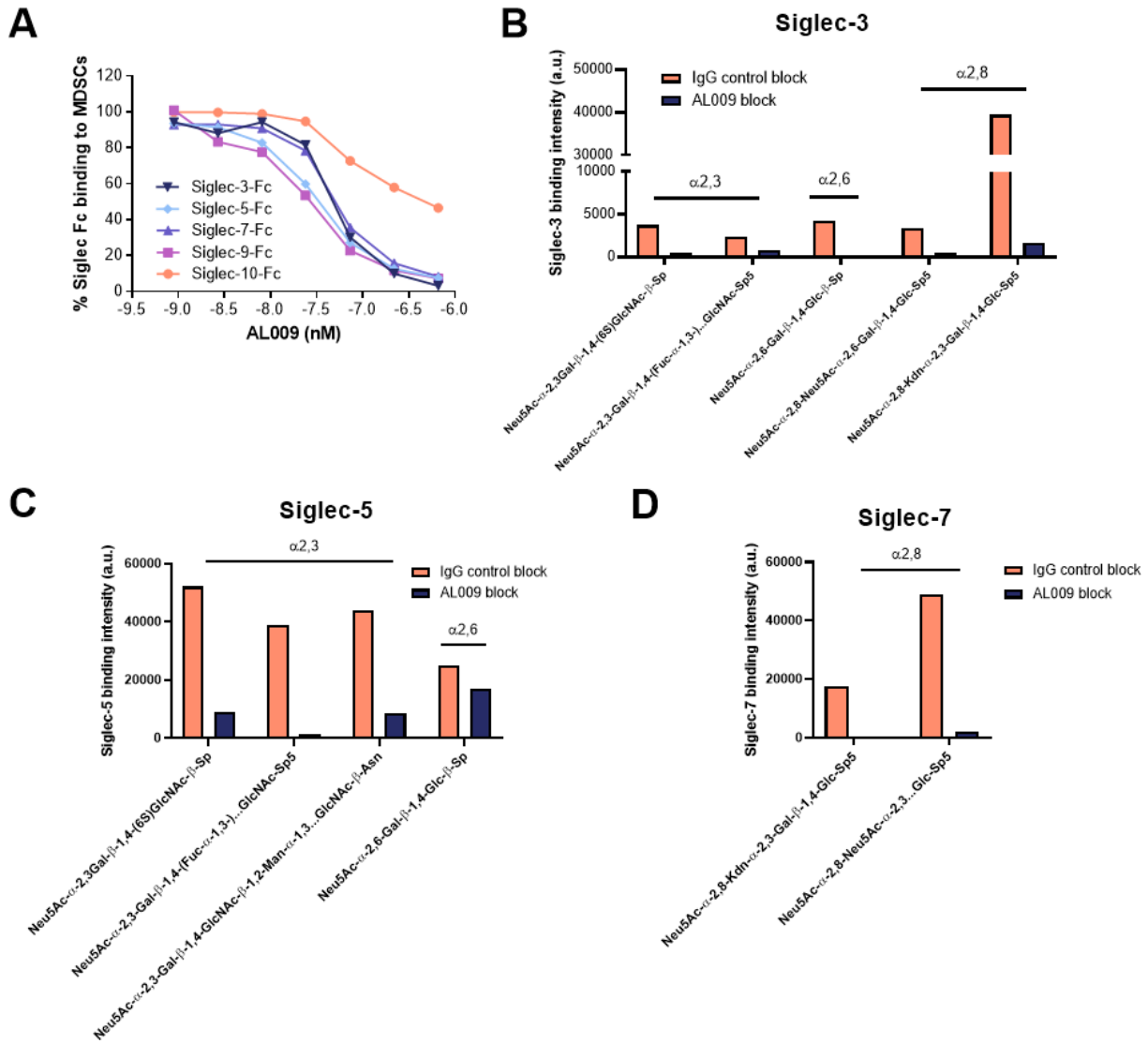

Fig. 1. AL009 blocks binding of inhibitory Siglec receptors and their ligands. (**A**) AL009 blocked binding of Siglec-3, -5, -7, -9, and -10 from binding to MDSCs in a dose-dependent manner. (**B-D**) In a glycan array containing over 100 sialic acids, AL009 blocked Siglec-3, -5, and -7 from binding their respective ligands. Fc, fragment crystallizable; MDSCs, myeloid-derived suppressor cells; Siglec, sialic acid–binding immunoglobulin-type lectin.

AL009 reprograms MDSCs

211 The phenotypic effect of AL009 blocking recognition between inhibitory Siglecs and their
212 ligands was assessed by incubating MDSCs with AL009 and evaluating cell surface markers,
213 cytokines, and chemokines. AL009 treatment resulted in a dose-dependent increase in immune
214 activation marker CD86 and a dose-dependent decrease in the immunosuppressive macrophage
215 marker CD163, consistent with reprogramming of MDSCs (Fig. 2A, 2B). Further, TNF
216 production was increased in a dose-dependent manner (Fig. 2C). In order to gain a greater
217 understanding of the reprogramming effect of AL009 on MDSCs, RNAseq analysis was
218 performed on MDSCs after AL009 treatment. AL009 induced robust expression of cytokines,
219 chemokines, and co-stimulatory molecules compared to isotype control in MDSCs (Fig. 2D).

220 We considered whether the reprogramming effect of AL009 treatment was specific to the
221 Siglec-9 ECD portion of the molecule. To evaluate this, MDSCs were treated with Siglec-3, -5, -
222 7, -9, or -10 ECD-Fc fusions and the reprogramming effect was assessed. The Siglec-9–mIgG
223 fusion resulted in the largest increase in activation markers CD86 and CD40 and the largest
224 reduction in suppressive macrophage markers CD163 and CD206 (Fig. S2A-D). The Siglec-9–
225 mIgG fusion was also the only Siglec-Fc fusion that induced a dose-dependent increase in CCL4
226 production by MDSCs, consistent with reprogramming of these cells (Fig. S2E).

227 Next, we examined whether AL009 was able to rescue MDSC suppression of T cells in a co-
228 culture system. MDSCs were treated with ligand-blocking antibodies against Siglec-3, -7, or -9,
229 a combination of all 3 antibodies, or AL009 prior to co-culture with activated T cells. The
230 amount of IFNɣ produced by the T cells was reduced in the presence of MDSCs and was not
231 rescued by any treatment except AL009 (Fig. 2E). In addition to increasing IFNɣ production in T
232 cells, we tested AL009's impact on T cell proliferation. After treatment with increasing
233 concentrations of AL009, T cell proliferation was quantified, with a half maximal effective

concentration of 1 to 2 nM AL009 (Fig. S3). Overall, AL009 is effective at potently repolarizing MDSCs, resulting in phenotypic changes consistent with a proinflammatory response and relief of T cell inhibition.

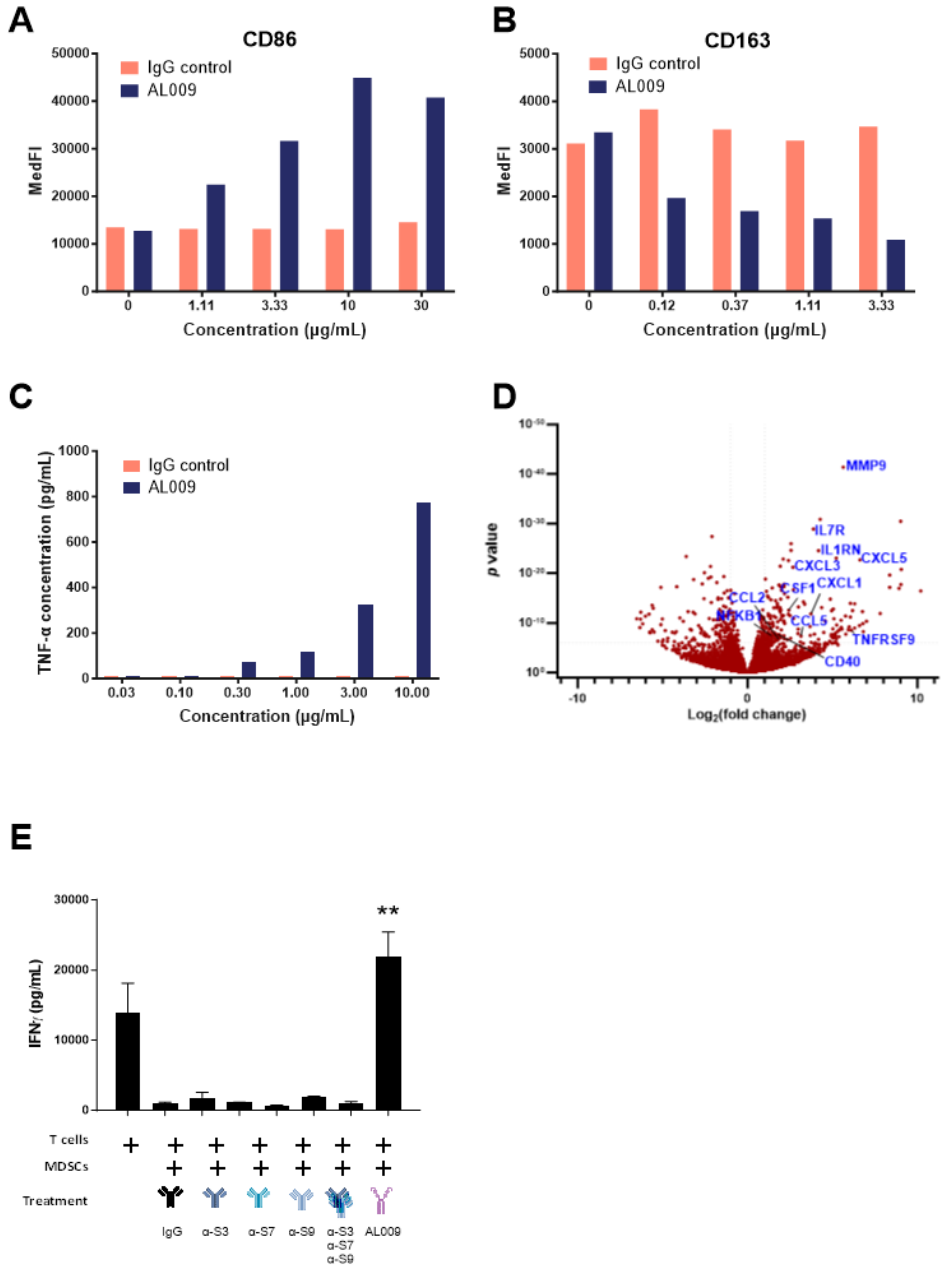

Fig. 2. AL009 repolarizes suppressive MDSCs. AL009 (**A**) enhanced CD86, (**B**) repressed CD163, and (**C**) induced TNF secretion after treatment on MDSCs. (**D**) AL009 treatment of MDSCs led to robust changes in gene expression. (**E**) AL009 rescued T cells suppressed by

241 MDSCs in a co-culture system. Error bars represent SEM. IFNɣ, interferon gamma; MDSCs,
242 myeloid-derived suppressor cells; MedFI, median fluorescence intensity; Siglec, sialic acid–
243 binding immunoglobulin-type lectin. $^{**}p < 0.01$, 2-sided t-test.

244

245 **AL009 activity depends on the ECD and Fc regions**

246 We hypothesized that both the Siglec-9 ECD and engineered Fc regions of AL009 were
247 important for the function of the molecule. To determine the contribution of the Siglec-9 ECD
248 portion of AL009, we first created domain mutation constructs. Production of the chemokine
249 CCL5 was induced with AL009, but that effect was ablated when the Siglec-9 ECD portion of
250 AL009 was deleted (Fig. 3A). Next, the Siglec-9 ECD and Fc fusion portions of AL009 were
251 decoupled, and MDSCs were incubated with plate-bound IgG to engage Fcγ receptors (FcγRs),
252 with or without a soluble AL009 mutant consisting of only the Siglec-9 ECD, then analyzed for
253 TNF production as a marker of MDSC programming (Fig. 3B). FcγR engagement by increasing
254 concentrations of plate-bound IgG induced a low level of TNF that was enhanced by the addition
255 of Siglec-9 ECD (Fig. 3C). We next asked if the Siglec-9 ECD could augment a separate
256 activation signal beyond FcγRs. Soluble anti-TREM1 or anti-TREM2 agonist antibodies were
257 incubated with MDSCs at increasing concentrations in addition to Siglec-9 ECD. Anti-TREM1
258 and anti-TREM2 had very minimal effects on MDSCs alone, but the addition of a fixed amount
259 of Siglec-9 ECD resulted in increased secretion of TNF in combination with TREM1 or TREM2
260 antibodies (Fig. 3D). These results demonstrate that Siglec-9 ECD alone is active and synergizes
261 with an activation signal in order to reprogram MDSCs.

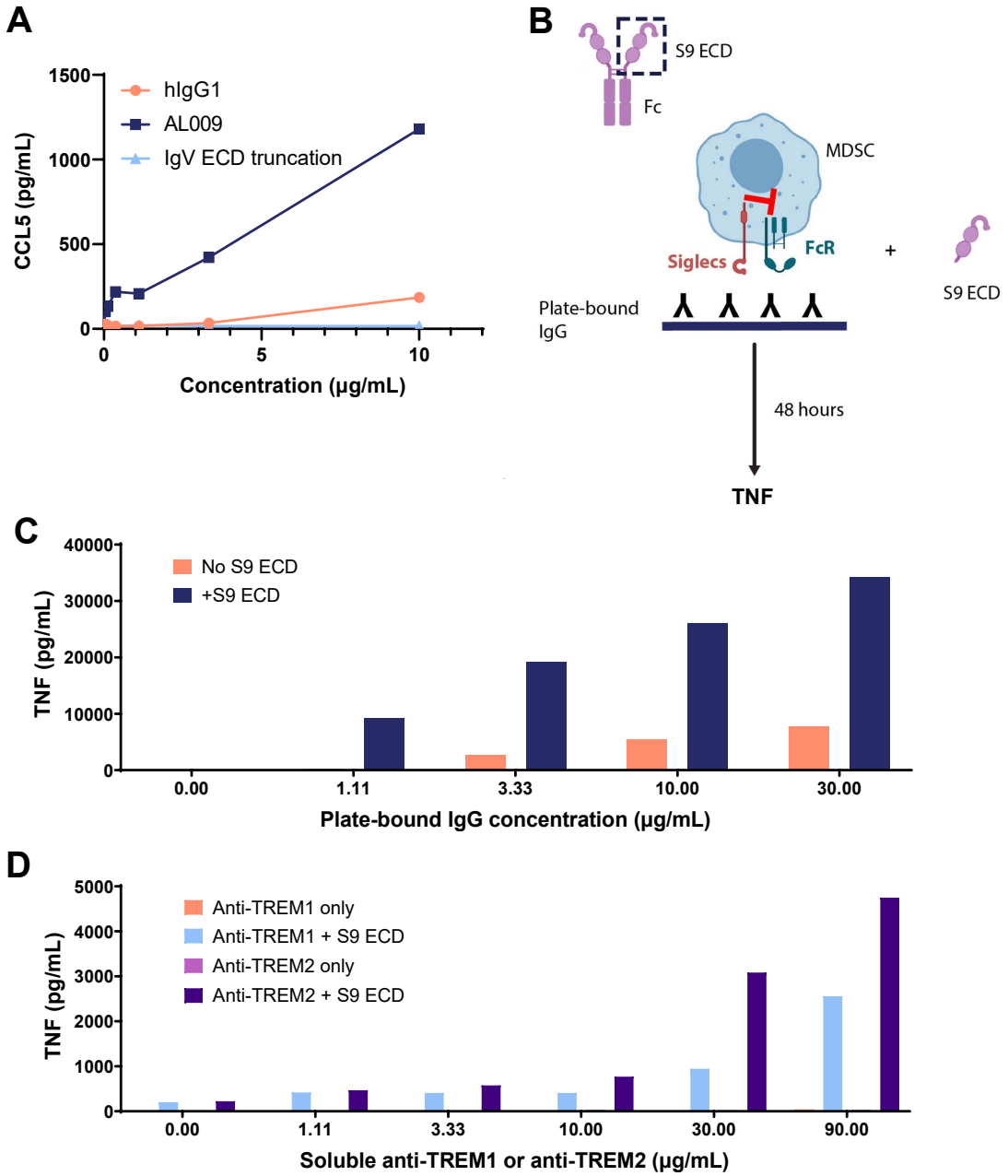

Fig. 3. The Siglec-9 ECD relieves immune suppression in the presence of an activating signal. (**A**) Truncation of the ECD domain of AL009 ablated its ability to induce CCL5. (**B**) Schematic of experimental setup. (**C**) Levels of TNF produced by MDSCs upon IgG cross-linking were increased in the presence of Siglec-9 ECD. (**D**) Levels of TNF produced by MDSCs were not induced by anti-TREM1 or anti-TREM2 alone but were induced when Siglec-9 ECD

268 was present. ECD, extracellular domain; Fc, fragment crystallizable; MDSCs, myeloid-derived
269 suppressor cells; MedFI, median fluorescence intensity; Siglecs, sialic acid–binding
270 immunoglobulin-type lectins.

271

272 The contribution of the Fc portion of AL009 was also investigated. The ability of AL009 to
273 relieve T cell suppression in an MDSC–T cell co-culture assay was greatly reduced when the Fc
274 portion of AL009 was silenced via mutations that ablate binding to FcγRs (Fig. 4A). To further
275 examine the contribution of the Fc portion of AL009 in binding MDSCs, dissociation constants
276 on cells were determined. The dissociation constant for AL009 when incubated with MDSCs
277 was 1.3 nM. However, when non-Fc receptor–expressing cells were used in place of MDSCs,
278 binding was much weaker (Kd = 220 nM). Similarly, when the Fc portion of AL009 was
279 silenced, binding to MDSCs was greatly reduced (Kd = 97 nM). In order to determine which Fc
280 gamma receptors were important for AL009 function, the ability of AL009 to increase CD86
281 expression at the cell surface, as a marker of MDSC reprogramming, was assessed in the
282 presence of antibodies against FcγRIIa, FcγRIIb, or a combination of FcγRIIa and FcγRIIb. The
283 N325S/L328F (NSLF) mutation contained within the Fc portion of AL009 prevents binding to
284 FcγRIIIa and FcγRIIIb; therefore, as expected there was no effect when MDSCs were incubated
285 with an FcγRIII blocking antibody prior to AL009 treatment. FcγRIIa blockade reduced AL009
286 activity, while FcγRIIb had no effect. Consistent with these results, the combination of FcγRIIa-
287 and FcγRIIb-blocking antibodies was equivalent to FcγRIIa blockade alone (Fig. 4B). Taken
288 together, these results suggest FcγRIIa is necessary for AL009 activity on MDSCs.

289

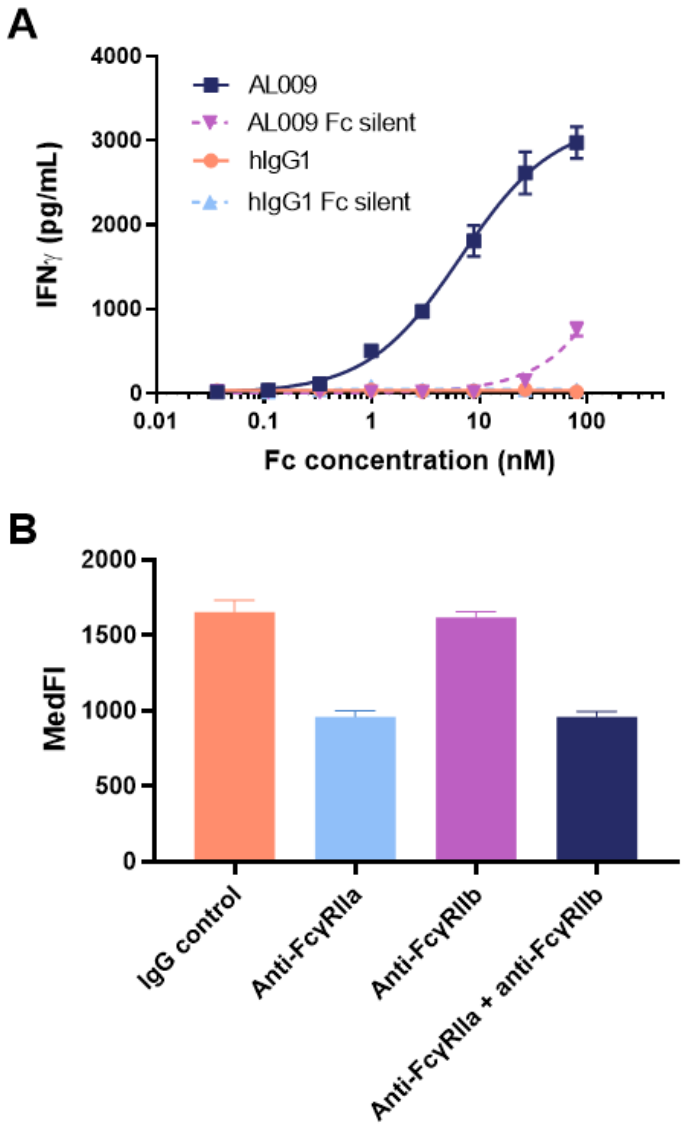

290

291 **Fig. 4. AL009 activity requires Fc receptor interactions.** (**A**) While AL009 was able to
292 reverse MDSC suppression and lead to higher levels of IFNɣ compared to control, AL009 Fc
293 silent was not able to elevate IFNɣ to the same extent. (**B**) FcɣRIIa was required for functional
294 activity of AL009 on MDSCs. Data are shown as mean ± SEM. Fc, fragment crystallizable;
295 IFNɣ, interferon gamma; MDSC, myeloid-derived suppressor cell; MedFI, median fluorescence
296 intensity.

297

298 **AL009 preferentially binds myeloid cells**

299 In whole human blood, binding of AL009 to a variety of immune cell subsets, including
300 monocytes, granulocytes, B cells, natural killer cells, T cells, and platelets, was assessed. AL009
301 preferentially bound monocytes compared to the other immune cell subsets tested (Fig. 5A). To
302 further elucidate cell subsets that are preferentially bound by AL009, donor blood samples were
303 used to compare AL009 binding to monocytes, macrophages, and MDSCs. The highest binding
304 observed was between AL009 and MDSCs, followed by non-activated M0 macrophages, and
305 then classically activated M1 macrophages (Fig. 5B).

306 AL009m, a mouse reactive surrogate for AL009 containing a mouse Fc, was created to assess the
307 activity of AL009 in vivo. A biodistribution study was performed with AL009m by fluorescently
308 labeling the molecule and then injecting it intravenously in mice. AL009m accumulation was
309 higher than the isotype control in macrophage-rich mouse tissue samples, such as liver and
310 spleen, while no difference between AL009m or isotype control was seen in other tissues, such
311 as heart and lung (Fig. 5C-5F). The results from both the whole human blood binding study and
312 biodistribution study provide evidence that AL009 preferentially binds myeloid cells both in
313 vitro and in vivo.

314

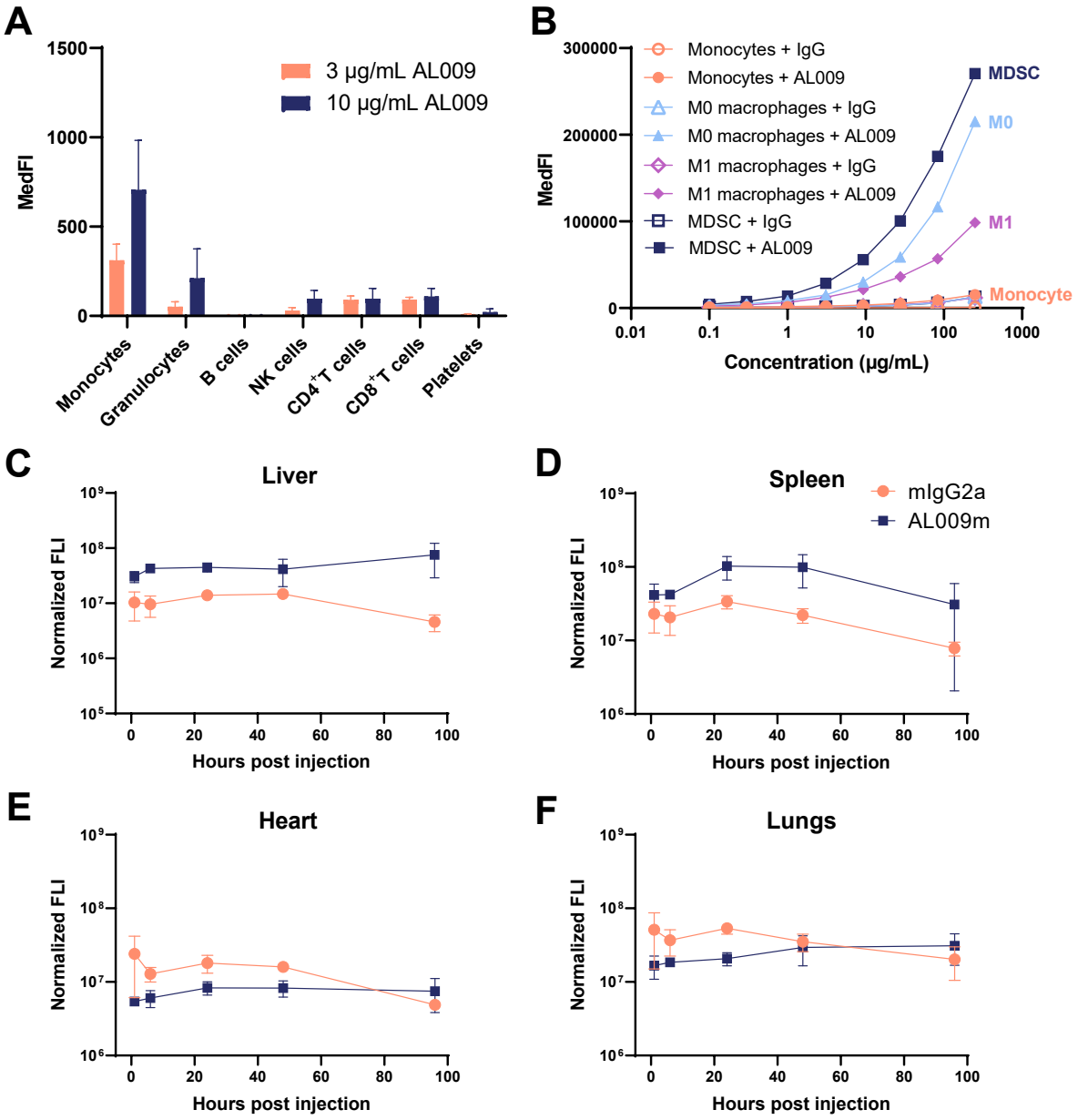

315

316 **Fig. 5. AL009 preferentially binds myeloid cells.** (**A**) In whole human blood, AL009

317 preferentially bound monocytes over granulocytes, B cells, NK cells, T cells, and platelets. (**B**)

318 AL009 preferentially bound MDSCs over other myeloid subsets, including M0 and M1

319 macrophages and monocytes. (**C-F**) In a biodistribution study in mice, AL009m accumulated in

320 macrophage-rich tissues, such as liver and spleen (n = 3 mice per timepoint). Error bars represent

321 SEM. FLI, fluorescence intensity; MDSC, myeloid-derived suppressor cell; MedFI, median
322 fluorescence intensity; NK, natural killer.

323

324 **AL009m demonstrates anti-tumor activity in mouse syngeneic tumor models**

325 Several syngeneic mouse tumor models were used to assess the anti-tumor efficacy of AL009m
326 in vivo. As a monotherapy, AL009m was tested in the E0771 triple negative breast cancer model.
327 Tumor volume was reduced and survival improved with AL009m treatment compared to isotype
328 control (Fig. 6A, 6B). To assess the impact of AL009m in combination with other therapies, the
329 B16-F10 intravenous injection model in combination with anti-TRP1 was utilized. In this model,
330 anti-TRP1 induces macrophage-mediated antibody-dependent cellular phagocytosis (ADCP) and
331 antibody-dependent cellular cytotoxicity (ADCC) of B16-F10 melanoma cells (24). Combination
332 treatment with AL009m and anti-TRP1 resulted in a significant reduction of lung nodules
333 compared to anti-TRP1 and isotype control (Fig. 6C). These results demonstrate that AL009m
334 can enhance ADCP/ADCC in vivo. To test the combination of AL009 with checkpoint
335 inhibitors, anti-PD-L1 was utilized along with AL009m in the MC38 and E0771 models. In both
336 models, anti-PD-L1 alone was not significantly different than isotype control, whereas
337 combination treatment with AL009m led to a significant reduction in tumor volume (Fig. 6D,
338 6E). Taken together, these efficacy results demonstrate that AL009m is active as a monotherapy
339 and in combination with an agent that induces ADCP/ADCC and the representative checkpoint
340 inhibitor anti-PD-L1.

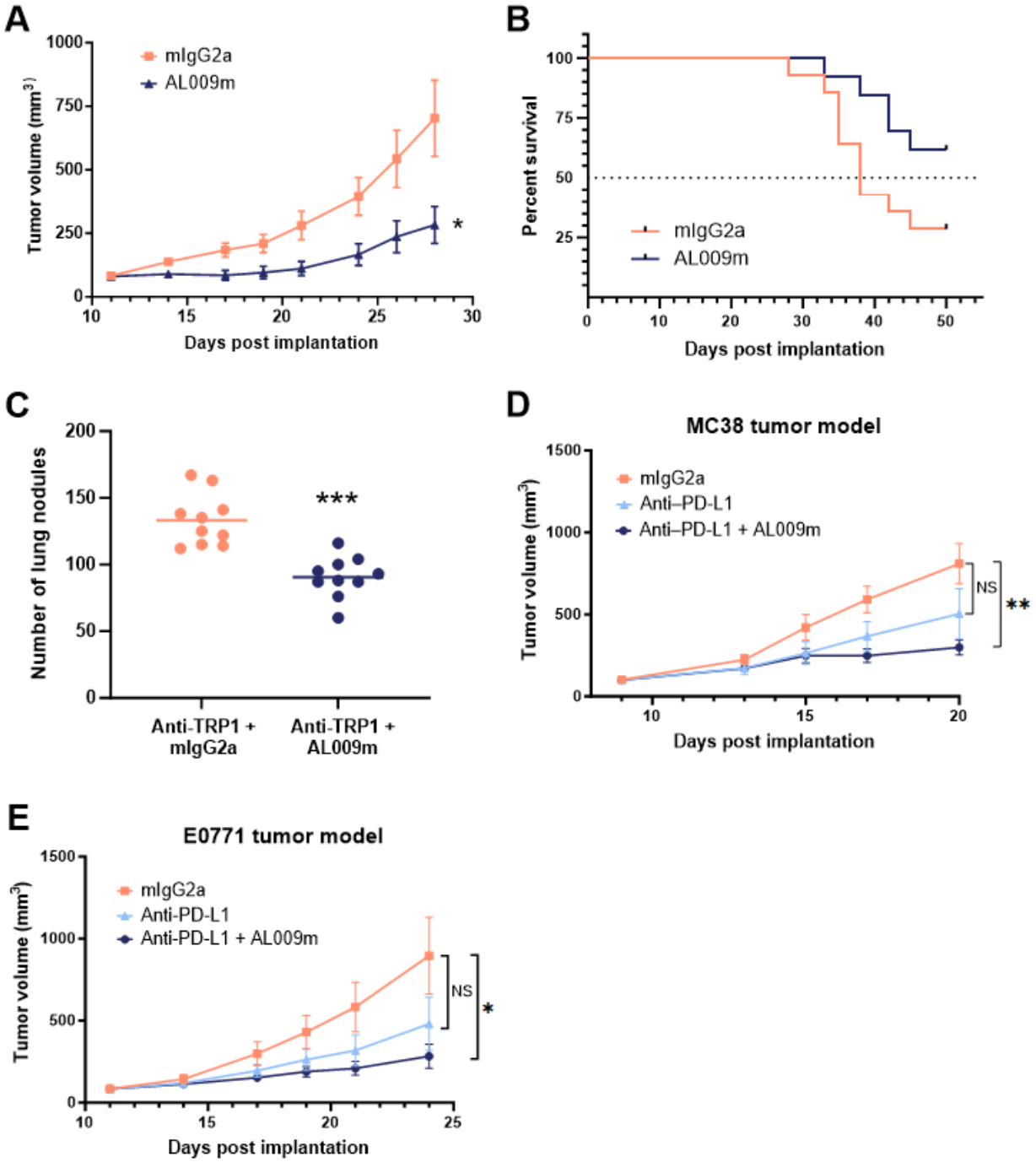

Fig. 6. **AL009m demonstrated anti-tumor activity in multiple mouse syngeneic tumor models.** (**A**) In the E0771 breast cancer model, AL009m treatment resulted in a significant reduction in tumor volume as well as (**B**) increased survival. (**C**) In the intravenous B16-F10 tumor model, combination treatment with anti-TRP1 and AL009 resulted in reduced lung

346 nodules. Line at mean. (**D**) In the MC38 tumor model, combination treatment with AL009m and
347 anti-PD-L1 resulted in reduced tumor volume. (**E**) In the E0771 breast cancer model,
348 combination treatment with AL009m and anti-PD-L1 showed a synergistic effect. (D-E) Data are
349 shown as mean ± SEM. *$p < 0.05$, **$p < 0.01$, ***$p < 0.001$, 2-sided t-test.

350

351 **Pharmacodynamic markers show enhanced immune activation in the tumor and spleen**
352 **following AL009 treatment**

353 To evaluate the pharmacodynamic effect of AL009m in the context of a tumor, spleen and tumor
354 samples from the E0771 mouse tumor models were analyzed by flow cytometry following
355 treatment with AL009m alone or in combination with anti-PD-L1. As a monotherapy, AL009m
356 treatment resulted in a significant decrease in Ly6C$^+$ cells, as a percentage of CD11b$^+$ cells,
357 indicating a decrease in MDSCs in tumor tissue (Fig. 7A). In spleen samples, an increase in
358 HLA-DR with AL009m treatment signaled activation of splenic macrophages (Fig. 7B). Further,
359 following AL009m treatment, there was a concurrent increase in activated CD4$^+$ cells in the
360 spleen, as measured by an enhanced percentage of CD69$^+$ cells (Fig. 7C). There was also an
361 increase in activated CD8$^+$ cells induced by AL009m that was further enhanced by anti-PD-L1
362 treatment, indicating a synergistic effect (Fig. 7D). In addition to the effects observed in the
363 tumor and spleen, AL009m also induced a dose-dependent increase in surface CD86 on
364 circulating monocytes (Fig. S4), similar to what was observed on human MDSCs following
365 AL009 treatment (Fig. 2A). The pharmacodynamic effect of AL009 was further evaluated in a
366 humanized mouse tumor model. In this humanized model, immunodeficient mice were engrafted
367 with human CD45$^+$ stem cells, implanted with a human A375 tumor weeks later, and treated
368 with AL009 approximately 2 weeks post implantation. Flow cytometry was used to analyze

369 tumor and spleen samples. Treatment with AL009 significantly decreased surface CD163 on
370 TAMs and splenic macrophages (Fig. 7E, 7F), demonstrating an in vivo reprogramming effect
371 consistent with the in vitro reprogramming observed with human MDSCs.

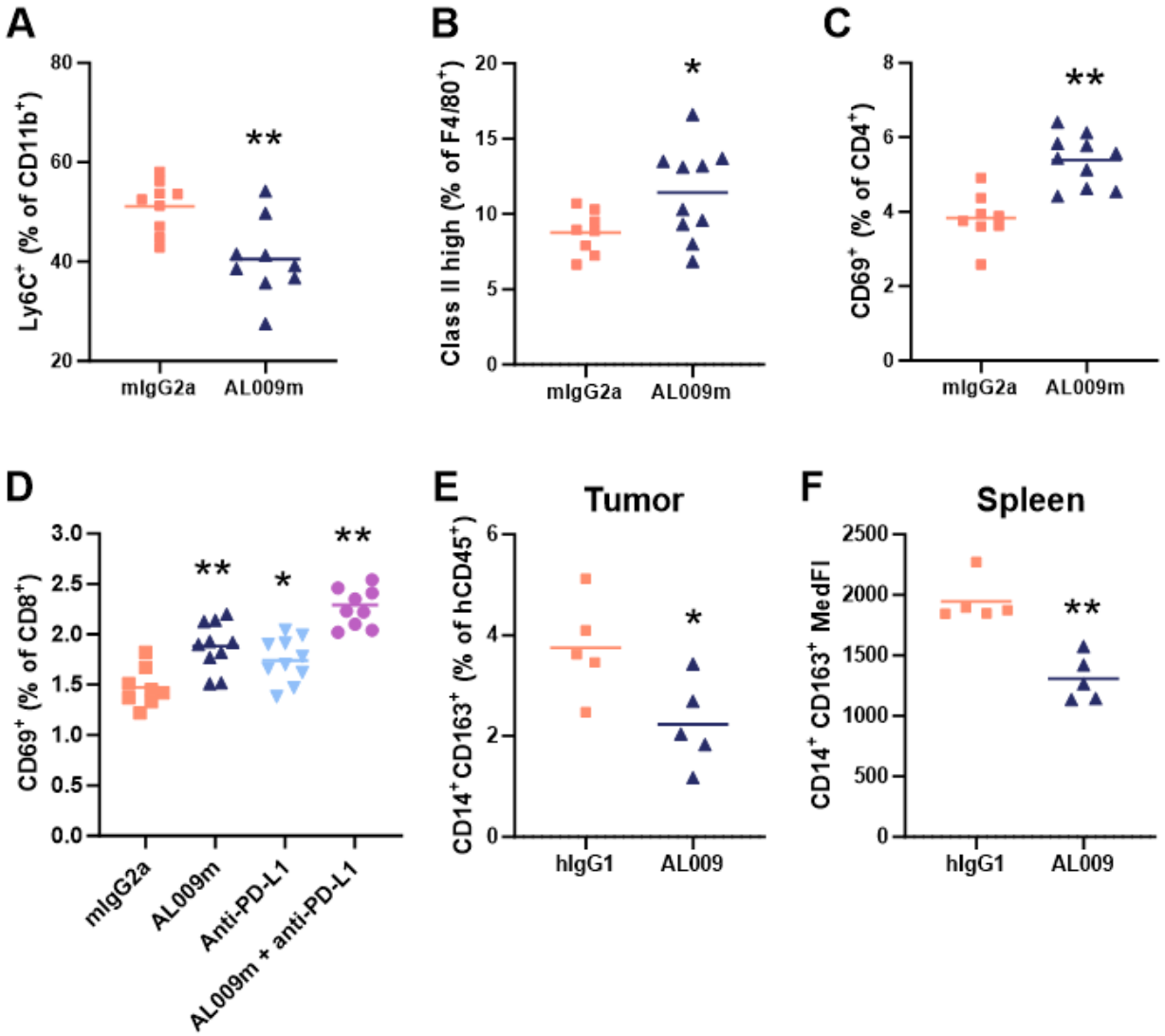

372

373 **Fig. 7. Pharmacodynamic biomarker data provides evidence that AL009m repolarizes**
374 **myeloid cells and activates T cells in vivo.** In the E0771 mouse tumor model, AL009m
375 treatment (**A**) decreased MDSCs in tumor tissue as shown by a decrease in Ly6C$^+$ cells, (**B**)
376 activated macrophages in spleen tissue as shown by increased Class II high cells, and (**C**)
377 activated CD4$^+$ T cells, as shown by an increase in CD69$^+$ cells. (**D**) CD8$^+$ T cells were also

378 increased with anti-PD-L1 treatment alone or in combination with AL009m treatment. (**E-F**) In a
379 humanized mice tumor model, AL009 treatment decreased levels of the pharmacodynamic
380 biomarker CD163, a marker for suppressive M2 macrophages, in the tumor and spleen. MDSC,
381 myeloid-derived suppressor cell; MedFI, median fluorescence intensity. Mean is shown. *$p <$
382 0.05, **$p < 0.01$, 2-sided t-test.
383

384 **DISCUSSION**

385 The current state of immunotherapy offers significant promise to treat cancer; however, while up
386 to half of all patients may be eligible for treatment with immunotherapy, less than 15% derive
387 clear benefit (25). TAMs heavily influence the TME and may comprise up to 50% of tumor
388 mass, which creates barriers to anti-tumor immunity and may underlie the resistance of some
389 patients to checkpoint inhibitors such as anti-PD1, anti-PD-L1, and anti-CTLA4 (26).
390 Consequently, an aspect of cancer immunotherapy drug development has shifted focus to
391 targeting the suppressive myeloid cells associated with tumors. There are currently TAM-
392 targeting therapeutics under investigation which aim to either deplete TAMs, block recruitment
393 of macrophages to the tumor, or reprogram TAMs to a proinflammatory phenotype (26, 27).
394 Depletion and blocking recruitment of macrophages disregard the anti-tumor potential of
395 creating reprogrammed, proinflammatory macrophages in the TME (27). Reprogramming TAMs
396 to a proinflammatory phenotype results in stimulation of cytotoxic T cells and tumor regression
397 in preclinical studies (26). Therapeutics aiming to reprogram TAMs may be effective as a
398 monotherapy or in synergy with checkpoint inhibitors (26, 28). As a TAM-reprogramming
399 therapeutic, AL009 provides two potential avenues for enabling immunotherapeutic activity: as a
400 monotherapy to drive macrophage modulation of the TME towards a more immune-responsive
401 environment, and in combination with checkpoint inhibitors to disrupt inherent immune-
402 mediated inhibition of the adaptive immune response. AL009 therefore represents a novel, multi-
403 functional therapeutic that has capacity for interrupting multiple negative regulatory signals in
404 TAMs with significant potential for treating cancer.

405 With its Siglec-9 ECD and engineered Fc region, AL009 targets immune cells to widely block
406 inhibitory signaling from Siglec receptors, leading to reprogramming of suppressive

407 macrophages. Siglecs are responsible for regulating immune homeostasis, with inhibitory Siglecs
408 playing a critical role in dampening immune responses (4, 8). The data from our experiments
409 confirm the ability of the Siglec-9 ECD of AL009 to bind sialic acid ligands of not only Siglec-9
410 but also other inhibitory Siglecs, thus broadly blocking immune-inhibitory Siglec–sialic acid
411 interactions. The disruption of this interaction allows anti-tumor activation signaling to proceed
412 (Fig. 8). The engineered Fc portion of AL009 facilitates localization to immune cells and
413 cooperative binding with the Siglec-9 ECD results in increased activity on innate immune cells.
414 (Fig. 8).

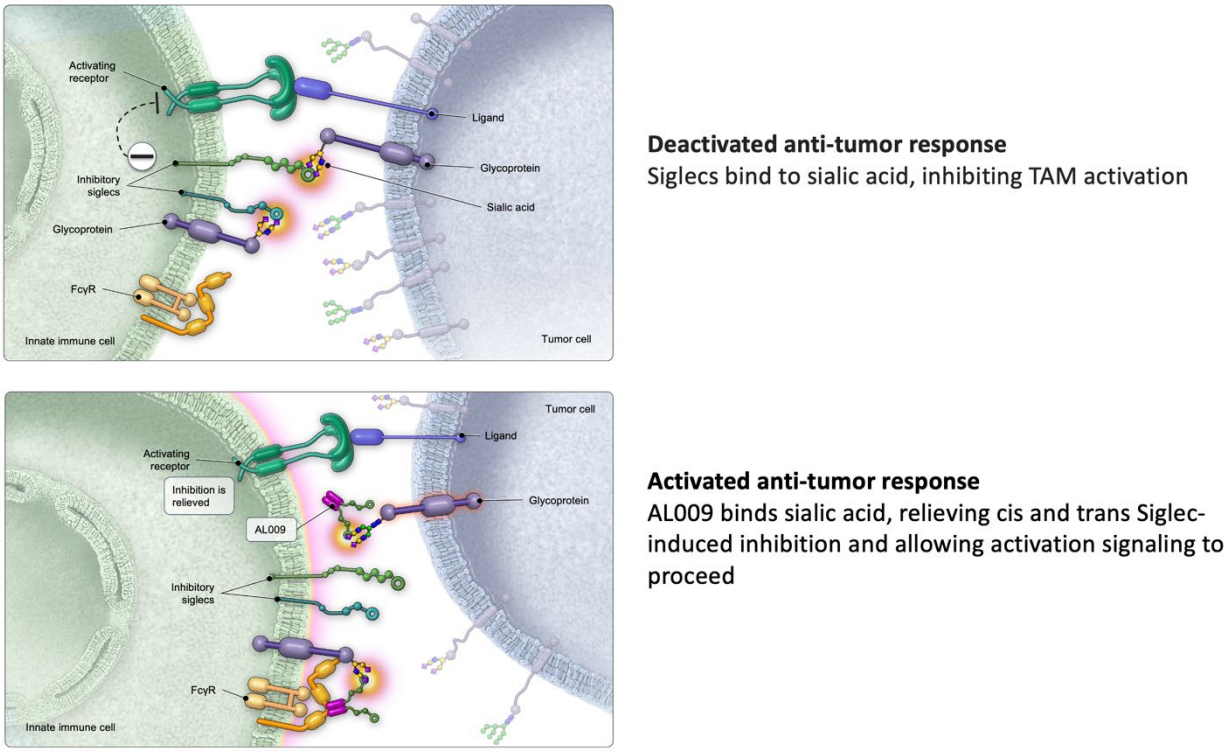

415

416 **Fig. 8. AL009 mechanism of action.** AL009 consists of an extracellular Siglec domain and an
417 engineered Fc portion for immune cell targeting. The Siglec portion of AL009 binds sialic acid
418 ligands in a cis or trans fashion, relieving Siglec-mediated immune suppression. FcγR, Fcγ
419 receptor.

420

421 Overall, AL009 is a differential approach to test the therapeutic hypothesis that TAM
422 reprogramming is an effective method of generating an anti-tumor effect in humans. Thus far,
423 pre-clinical studies have not identified any significant toxicology signals. In addition, serum and
424 immune cell pharmacodynamic biomarkers have been identified, and immunohistochemistry
425 companion diagnostic development is underway. Taken together, these preclinical results support
426 clinical testing of the safety and efficacy of AL009.

427 **Acknowledgments:** Editorial support and publication assistance were provided by SCIENT
428 Healthcare Communications (Cedar Knolls, NJ, USA).

429 **References**

430 1. Crocker, P. R., J. C. Paulson, and A. Varki. 2007. Siglecs and their roles in the immune
431 system. *Nat. Rev. Immunol.* 7: 255-266.
432 2. Laubli, H., and A. Varki. 2020. Sialic acid-binding immunoglobulin-like lectins (Siglecs)
433 detect self-associated molecular patterns to regulate immune responses. *Cell Mol. Life*
434 *Sci.* 77: 593-605.
435 3. Dos Reis, J. S., I. Diniz-Lima, M. Santos, P. M. Barcelos, K. M. da Costa, R. D. C.
436 Valente, L. S. Chaves, L. P. de Campos, A. C. Dos Santos, R. G. Correia de Lima, D.
437 Decote-Ricardo, A. Morrot, J. O. Previato, L. Mendonca-Previato, C. G. Freire-de-Lima,
438 L. M. D. Fonseca, and L. Freire-de-Lima. 2023. The blessed union of glycobiology and
439 immunology: a marriage that worked. *Medicines (Basel)* 10.
440 4. Macauley, M. S., P. R. Crocker, and J. C. Paulson. 2014. Siglec-mediated regulation of
441 immune cell function in disease. *Nat. Rev. Immunol.* 14: 653-666.
442 5. Santegoets, K. C. M., P. R. Gielen, C. Bull, B. M. Schulte, E. D. Kers-Rebel, B. Kusters,
443 S. Bossman, M. Ter Laan, P. Wesseling, and G. J. Adema. 2019. Expression profiling of
444 immune inhibitory Siglecs and their ligands in patients with glioma. *Cancer Immunol.*
445 *Immunother.* 68: 937-949.
446 6. Paulson, J. C., M. S. Macauley, and N. Kawasaki. 2012. Siglecs as sensors of self in
447 innate and adaptive immune repsonses. *Ann. N. Y. Acad. Sci.* 1253: 37-48.
448 7. Rodriguez, E., S. T. T. Schetters, and Y. van Kooyk. 2018. The tumour glyco-code as a
449 novel immune checkpoint for immunotherapy. *Nat. Rev. Immunol.* 18: 204-211.
450 8. Laubli, H., S. C. Nalle, and D. Maslyar. 2022. Targeting the Siglec-sialic acid immune
451 axis in cancer: current and future approaches. *Cancer Immunol. Res.* 10: 1423-1432.

452 9. Murugesan, G., B. Weigle, and P. R. Crocker. 2021. Siglec and anti-Siglec therapies.
453 *Curr. Opin. Chem. Biol.* 62: 34-42.
454 10. Orekhov, A. N., V. A. Orekhova, N. G. Nikiforov, V. A. Myasoedova, A. V. Grechko, E.
455 B. Romanenko, D. Zhang, and D. A. Chistiakov. 2019. Monocyte differentiation and
456 macrophage polarization. *Vessel Plus* 3: 10.
457 11. Zhou, J., Z. Tang, S. Gao, C. Li, Y. Feng, and X. Zhou. 2020. Tumor-associated
458 macrophages: recent insights and therapies. *Front. Oncol.* 10: 188.
459 12. Kumar, V., S. Patel, E. Tcyganov, and D. I. Gabrilovich. 2016. The nature of myeloid-
460 derived suppressor cells in the tumor microenvironment. *Trends Immunol.* 37: 208-220.
461 13. Chen, Y., Y. Song, W. Du, L. Gong, H. Chang, and Z. Zou. 2019. Tumor-associated
462 macrophages: an accomplice in solid tumor progression. *J. Biomed. Sci.* 26: 78.
463 14. Lv, M., X. Zhuang, S. Shao, X. Li, Y. Cheng, D. Wu, X. Wang, and T. Qiao. 2022.
464 Myeloid-derived suppressor cells and CD68(+)CD163(+)M2-like macrophages as
465 therapeutic response biomarkers are associated with plasma inflammatory cytokines: a
466 preliminary study for non-small cell lung cancer patients in radiotherapy. *J. Immunol.*
467 *Res.* 2022: 3621496.
468 15. Cai, H., Y. Zhang, J. Wang, and J. Gu. 2021. Defects in macrophage reprogramming in
469 cancer therapy: the negative impact of PD-L1/PD-1. *Front. Immunol.* 12: 690869.
470 16. Qiu, S. Q., S. J. H. Waaijer, M. C. Zwager, E. G. E. de Vries, B. van der Vegt, and C. P.
471 Schroder. 2018. Tumor-associated macrophages in breast cancer: innocent bystander or
472 important player? *Cancer Treat. Rev.* 70: 178-189.

473 17. Xiao, N., X. Zhu, K. Li, Y. Chen, X. Liu, B. Xu, M. Lei, J. Xu, and H. C. Sun. 2021.
474 Blocking siglec-10(hi) tumor-associated macrophages improves anti-tumor immunity and
475 enhances immunotherapy for hepatocellular carcinoma. *Exp. Hematol. Oncol.* 10: 36.
476 18. Duan, Z., and Y. Luo. 2021. Targeting macrophages in cancer immunotherapy. *Signal*
477 *Transduct. Target. Ther.* 6: 127.
478 19. Viitala, M., R. Virtakoivu, S. Tadayon, J. Rannikko, S. Jalkanen, and M. Hollmen. 2019.
479 Immunotherapeutic blockade of macrophage Clever-1 reactivates the CD8(+) T-cell
480 response against immunosuppressive tumors. *Clin. Cancer Res.* 25: 3289-3303.
481 20. Georgoudaki, A. M., K. E. Prokopec, V. F. Boura, E. Hellqvist, S. Sohn, J. Ostling, R.
482 Dahan, R. A. Harris, M. Rantalainen, D. Klevebring, M. Sund, S. E. Brage, J. Fuxe, C.
483 Rolny, F. Li, J. V. Ravetch, and M. C. Karlsson. 2016. Reprogramming tumor-associated
484 macrophages by antibody targeting inhibits cancer progression and metastasis. *Cell Rep.*
485 15: 2000-2011.
486 21. La Fleur, L., J. Botling, F. He, C. Pelicano, C. Zhou, C. He, G. Palano, A. Mezheyeuski,
487 P. Micke, J. V. Ravetch, M. C. I. Karlsson, and D. Sarhan. 2021. Targeting MARCO and
488 IL37R on immunosuppressive macrophages in lung cancer blocks regulatory T cells and
489 supports cytotoxic lymphocyte function. *Cancer Res.* 81: 956-967.
490 22. Mantovani, A., P. Allavena, F. Marchesi, and C. Garlanda. 2022. Macrophages as tools
491 and targets in cancer therapy. *Nat. Rev. Drug Discov.* 21: 799-820.
492 23. Genard, G., S. Lucas, and C. Michiels. 2017. Reprogramming of tumor-associated
493 macrophages with anticancer therapies: radiotherapy versus chemo- and
494 immunotherapies. *Front. Immunol.* 8: 828.

495 24. Benonisson, H., H. S. Sow, C. Breukel, J. Claassens, C. Brouwers, M. M. Linssen, M. F.
496 Fransen, M. Sluijter, F. Ossendorp, T. van Hall, and J. S. Verbeek. 2018. High
497 FcgammaR expression on intratumoral macrophages enhances tumor-targeting antibody
498 therapy. *J. Immunol.* 201: 3741-3749.
499 25. Haslam, A., and V. Prasad. 2019. Estimation of the percentage of US patients with cancer
500 who are eligible for and respond to checkpoint inhibitor immunotherapy drugs. *JAMA*
501 *Netw. Open* 2: e192535.
502 26. Pathria, P., T. L. Louis, and J. A. Varner. 2019. Targeting tumor-associated macrophages
503 in cancer. *Trends Immunol.* 40: 310-327.
504 27. Kumari, N., and S. H. Choi. 2022. Tumor-associated macrophages in cancer: recent
505 advancements in cancer nanoimmunotherapies. *J. Exp. Clin. Cancer Res.* 41: 68.
506 28. Xiang, X., J. Wang, D. Lu, and X. Xu. 2021. Targeting tumor-associated macrophages to
507 synergize tumor immunotherapy. *Signal Transduct. Target Ther.* 6: 75.
508

509 **Footnotes:**

510 [1]This work was supported by Alector, Inc.

511 [2]Corresponding author. Email: sam.nalle@alector.com. Telephone: 773-454-1434.

512 Abbreviations used in this article:

513 ADCC, antibody-dependent cellular cytotoxicity

514 ADCP, antibody-dependent cellular phagocytosis

515 ECD, extracellular domain

516 Fc, fragment crystallizable

517 FcγR, Fcγ receptor

518 IFNɣ, interferon gamma

519 MDSC, myeloid-derived suppressor cell

520 MedFI, median fluorescence intensity

521 Siglec, sialic acid–binding immunoglobulin-type lectin

522 TAM, tumor-associated macrophage

523 TME, tumor microenvironment

524 TREM-1, triggering receptor expressed on myeloid cells 1

525 TREM-2, triggering receptor expressed on myeloid cells 2

526 **Competing interests:** All authors are shareholders of Alector, Inc., or were shareholders of

527 Alector, Inc., when the studies were being conducted. SCN and SL are inventors on a patent

528 application related to this work.